# Estimating cause- and size- specific mortality hazard rates using mark-recapture-recovery data

Chloé R. Nater*[a], Yngvild Vindenes[a], Per Aass[b], Diana Cole[c], Øystein Langangen[a], S. Jannicke Moe[d], Atle Rustadbakken[e], Daniel Turek[f], L. Asbjørn Vøllestad[a] and Torbjørn Ergon[a]

[a]Centre for Ecological and Evolutionary Synthesis (CEES), Department of Biosciences, University of Oslo, Oslo, Norway

[b]Zoological Museum, The Natural History Museums and Botanical Garden, University of Oslo, Oslo, Norway

[c]School of Mathematics, Statistics and Actuarial Science, University of Kent, Canterbury, England

[d]Norwegian Institute for Water Research (NIVA), Oslo, Norway

[e]The Freshwater Fish Administration, County Governor of Hedmark, Hamar, Norway

[f]Department of Mathematics and Statistics, Williams College, Williamstown, Massachusetts, United States

Running headline: Cause- and size-specific mortality

*c.r.nater@ibv.uio.no

# Abstract

Estimating survival using data on marked individuals is a key component of population dynamics studies resulting management and conservation decisions. When human impacts on populations are considerable, such decisions require not only estimating survival but also quantifying how much mortality is due to anthropogenic versus natural causes. This is of particular importance when individuals vary in their vulnerability to different causes of mortality due to, for example, their body size, developmental stage, or reproductive state. In this study we used multistate mark-recapture models to estimate the effects of individual body size on harvest- and background mortality risks of large freshwater brown trout (*Salmo trutta*). In doing so, we accounted for additional individual differences in vulnerability to cause-specific mortality by distinguishing individuals passing a hydroelectric dam on their spawning migration from those that reproduced below the dam instead and further investigate temporal patterns of and correlations among mortality hazard rates over 50 years. We found that harvest mortality was highest for intermediate-sized trout, and outweighed background mortality for almost the entire observed size range of trout. For trout spawning above the dam, background mortality decreased for larger body sizes and at lower river discharge. Both mortality causes, as well as the probability of spawning above the dam, varied substantially over time but a trend was evident only for fishers' reporting rate, which decreased from an average of 80% to only 10% over half a century. Our model demonstrates how continuous size effects can be integrated into analyses of cause-specific mortality by using a novel parameterisation with hazard rates. This allowed us to estimate effects of both size and environment on harvest- and background mortality with-

out confounding, and provided an intuitive way to estimate temporal patterns within and correlation among the mortality sources. In combination with computationally fast custom MCMC solutions this modelling framework provides unique opportunities for studying individual heterogeneity in cause-specific mortality using mark-recapture-recovery data.

## Keywords

Bayesian statistics, dam, harvesting, hazard rate, mark-recapture, mortality, trout.

# Introduction

Population dynamics - particularly of long-lived species - are often very sensitive to changes in mortality (Sæther and Bakke 2000, Fujiwara and Caswell 2001). Mortality itself can have a wide variety of causes (*e.g.* starvation, predation, disease, harvest), and vulnerability to cause-specific mortality depends strongly on individual factors such as age or life stage (Ronget et al. 2017). As a consequence, population-level responses to changes in mortality may vary greatly depending on the underlying cause, and disentangling different causes of mortality may thus provide insights crucial for population management and conservation (Williams et al. 2002). This is particularly important in populations where significant mortality is linked to human activity; in such cases, knowledge about the relative impact of human-induced mortality and its potential effect on other sources of mortality is crucial for developing sustainable and successful harvest- or culling strategies (Hilborn and Walters 2013, Koons et al. 2014).

Studies of marked individuals constitute a highly valuable source of demographic data for wild animal populations and are crucial for estimating survival, as well as cause-specific mortalities. The recovery of a dead marked animal often provides information on the cause of death. For example, it was evident from the recovery of radio-collared European hares (*Lepus eruopaeus*) whether they had died due to hunting, predation, or other causes (Devillard and Bray 2009). Similarly, location and examination of recovered white storks (*Ciconia ciconia*) allowed identifying whether they had died from collision with a power line, or due to other causes (Schaub and Pradel 2004). However, unless animals are marked with radio- or satellite transmitters, most dead individuals will not be found, and this imperfect detection needs to be accounted for when estimating survival or mortality parameters. Moreover, when considering multiple mortality causes, detection probability frequently depends on the cause of mortality, and some causes of mortality may not be observable at all. This is usually the case for natural mortality when dead recoveries are exclusively based on the reports of hunters or fishers (*e.g.* Servanty et al. 2010, Koons et al. 2014).

Schaub and Pradel (2004) developed a multistate mark-recapture-recovery framework that allows to separately estimate mortality from different causes while accounting for cause-dependent detection probabilities. Specifically, cause-specific mortalities are estimated as transitions from an "alive" state to several "dead from cause of interest" states. When this framework is extended to also include multiple "alive" states, it becomes possible to estimate differences in vulnerability to cause-specific mortality depending on, for example, an individual's life-stage (*e.g.* juveniles vs. adults, Schaub and Pradel 2004) or location (Fernández-Chacón et al. 2015). Such group-level differences in mortality can be tremendous and account-

ing for them is crucial for modelling population dynamics (Ronget et al. 2017). However, in addition to that, vital rates and population dynamics are often also strongly affected by individual differences in continuous, dynamic traits such as body size (De Roos et al. 2003, Vindenes and Langangen 2015). Particularly in species that are harvested and/or have indeterminate growth (*e.g.* fish species), cause-specific mortality is expected to depend strongly on body size. Fernández-Chacón et al. (2017) demonstrated this by estimating cause-specific mortalities for different sizes of Atlantic cod (*Gadus morhua*). However, they did so by lumping individuals into either of two size classes ("small" or "large"), thus foregoing the possibility of investigating the continuous relationship between body size and mortality from different causes. While interesting and informative on its own, knowledge about the relationships between continuous traits and vital rates like mortality are also invaluable for studying dynamical processes at the population level, (*e.g.* using integral projection models, Ellner and Rees 2006).

In this study, we extended the framework of multiple mortality cause mark-recapture models to include a continuous individual- and time-varying trait (body size) as a predictor of vulnerability within different groups of individuals. By modelling survival and mortality probabilities via cause-specific mortality hazard rates (Ergon et al. 2018) we estimated the effects of body size on, as well as among-year environmental variation in, different mortality causes without confounding. We then used this extended model to investigate size-dependence of and temporal patterns in harvest and background mortality of adult brown trout (*Salmo trutta*) over half a century (1966 - 2016).

Migratory salmonid fishes - such as piscivorous brown trout - are extensively studied due to their ecological, cultural and economical value (Drenner et al. 2012).

Nonetheless, contrary to other parts of the life history, relatively little is known about the mortality of adults residing in the sea or large lakes (Piccolo et al. 2012). Many salmonid populations are heavily impacted by human activity not only in the form of harvesting but also through pollution, fish farming, habitat fragmentation, and hydro-electrical power production (dams) in rivers (Aas et al. 2010). Our study population of migratory brown trout (hereafter "Hunder trout" or just "trout") inhabits a river-lake system in Eastern Norway and has been a popular target for fishing for decades due to its large body size. The spawning river is dammed, and trout migrating to spawning grounds above the dam face additional risks linked to passing the dam on their up- and downriver migrations. These risks are likely associated with individual body size as well as environmental conditions, and can be avoided entirely if trout instead use the spawning grounds below the dam. Each individual's spawning location thus determines its exposure and vulnerability to some sources of mortality (*e.g.* those related to the dam), and we accounted for this heterogeneity by modelling cause-specific mortality hazard rates not only as a function of body size, but also as dependent on whether individuals migrate past the dam to spawn. By fitting the resulting model to a unique 50-year time-series of recaptures and recoveries of marked trout, we investigated the detailed effects of individual- (size, spawning location) and environmental (river discharge) factors on the vulnerability of adult trout to mortality due to harvest, passage of a hydroelectric dam, and natural causes, as well as on the probability of using a fish ladder within the dam to access upriver spawning areas. Additionally, we extended our analyses to also (1) investigate potential early life impacts of hatchery-rearing, since part of the population consist of stocked fish, and (2) estimate the temporal correlation of harvest- and background mortality.

# Materials and methods

## STUDY SYSTEM AND DATA

We studied a population of landlocked migratory brown trout inhabiting the lake Mjøsa and its main inlet river, Gudbrandsdalslågen, in Eastern Norway. These trout have a life history that is similar to that of Atlantic salmon (*Salmo salar*)(Aass et al. 1989): juveniles are hatched in the river and spend on average 4 years there before smolting and migrating to the lake. They typically mature after 2 - 3 years of piscivorous diet and fast growth in the lake, and from that point on migrate up the river to spawn every other year (usually in August/September, Figure 1). The adult trout population consists of wild-born trout and stocked (first-generation hatchery-reared) trout which are released into the river and lake as smolts but then follow the same general life history. Shortly after the river was dammed in the 1960's, a fish ladder was installed to enable mature trout to reach their historical spawning grounds above the dam. There are spawning grounds downriver of the dam as well (Aass et al. 1989), and an individual trout's spawning location is thus linked to whether or not it uses the fish ladder to travel upriver. This - in turn - is influenced by body size and hydrological conditions (Haugen et al. 2008).

From 1966 to 2016 a trap was operated within the fish ladder, allowing for all trout passing the ladder to be captured, measured and individually marked. Thus, all adult trout were marked when they used the fish ladder on an upriver spawning migration for the first time, and were recaptured on subsequent spawning migrations given that they had survived and were passing the ladder again (usually every other year, Figure 1). Over the 50-year time period, 14,890 adult trout were

marked and 2,152 of these were recaptured in the ladder later. Since the population has been exposed to fishing over the entire time period, an additional 2,306 marked trout were reported dead by fishers. For more details on the marking scheme, sampling protocol, and resulting data from the mark-recapture-recovery study, see Moe et al. (2018).

In the present study we performed mark-recapture analyses over intervals of two years, as estimating parameters for spawning and non-spawning years separately proved problematic (due to trout being unobservable in non-spawning years, Figure 1). We thus summarised the data into individual capture histories $y_{i,t}$, in which each time index $t$ corresponds to a two-year time step (interval from current spawning year to next spawning year). For each time step within those capture histories, we coded three types of observations: 1 = alive and captured in the ladder, 2 = dead from harvest and reported, and 3 = not observed. Upriver spawning migrations occur over the period from June to November but peak in August (Figure S1.1), and we set $y_{i,t} = 1$ when an individual was captured in the fish ladder in any month during time interval $t$. Harvest of trout happens year-round (Figure S1.1) and if an individual was harvested and reported at any point during interval $t$ we set $y_{i,t} = 2$, unless (a) the individual had also been caught in the fish ladder during interval $t$ or (b) the harvest happened after August of the second year within the interval $t$. If either (a) or (b) was the case, we moved the harvest observation to the next interval such that $y_{i,t+1} = 2$. Furthermore, we excluded all individuals that did not follow a strictly biennial spawning cycle (1.5% of all individuals), did not have a single size measurement taken (7.1%), or were of unknown origin (wild vs. stocked, <1%). The analyses presented here are based on the remaining 12,875 capture histories containing 1,588 trap recaptures and 2,252 harvest recoveries.

# MODEL FORMULATION

## General model structure

Survival and deaths due to certain causes represent mutually exclusive events and can thus be incorporated into multistate mark-recapture frameworks (Lebreton et al. 1999). When explicitly including not only "alive" but also (observable) cause-specific "newly dead" states, the probability of transitioning from state "alive" to state "newly dead from cause X" represents the probability of dying from cause X (Schaub and Pradel 2004, Servanty et al. 2010). In the trout study population, deaths due to harvest may be reported by fishers and are thus clearly distinguishable from deaths due to other causes. Individuals in any alive state $n$ can therefore remain alive with survival probability $S_n$ or transition to states "newly dead from harvest" (state 3) or "permanently dead" (state 4) with probabilities $\Psi_n^H$ and $\Psi_n^O$ respectively (Figure 2). The "permanently dead" state here represents all unobservable dead individuals, which also include those that have recently died from causes other than harvest. Furthermore, we make a distinction between individuals that start the time interval by spawning above versus below the dam. Spawning location may have a considerable effect on mortality, as individuals that spawn above the dam need to pass this obstacle on both the upriver- and downriver spawning migration. Consequently, we included two "alive" states in our model: "spawning upriver" (state 1) and "spawning downriver" (state 2). Individuals in each spawning state $n$ have a survival probability $S_n$, a probability of dying due to harvest $\Psi_n^H$, and a probability of dying due to other causes $\Psi_n^O$. Additionally, there is a probability of using the fish ladder, $p$, which links the two alive states and is assumed to be independent of previous spawning location (Figure 2). The

resulting model can be expressed with the state transition matrix

$$
\begin{array}{cc|cccc}
 & & \multicolumn{4}{c}{states\ (t+1)} \\
 & & \mathbf{1} & \mathbf{2} & \mathbf{3} & \mathbf{4} \\
\hline
states\ (t) & \mathbf{1} & S_{1,i,t}p_{i,t+1} & S_{1,i,t}(1-p_{i,t+1}) & \Psi^{H}_{1,i,t} & \Psi^{O}_{1,i,t} \\
 & \mathbf{2} & S_{2,i,t}p_{i,t+1} & S_{2,i,t}(1-p_{i,t+1}) & \Psi^{H}_{2,i,t} & \Psi^{O}_{2,i,t} \\
 & \mathbf{3} & 0 & 0 & 0 & 1 \\
 & \mathbf{4} & 0 & 0 & 0 & 1
\end{array}
$$

The elements of this matrix represent the probabilities of any individual $i$ in a given state (rows) transitioning to another state (columns) over the time interval from $t$ to $t+1$. As such, all probabilities within a given row sum to 1.

Similarly, these same states 1-4 are linked to the three types of observations in the data through a matrix of observation probabilities (columns) given a state (rows):

$$
\begin{array}{cc|ccc}
 & & \multicolumn{3}{c}{observations\ (t)} \\
 & & \mathbf{1} & \mathbf{2} & \mathbf{3} \\
\hline
states\ (t) & \mathbf{1} & 1 & 0 & 0 \\
 & \mathbf{2} & 0 & 0 & 1 \\
 & \mathbf{3} & 0 & r_t & 1-r_t \\
 & \mathbf{4} & 0 & 0 & 1
\end{array}
$$

where 1 = alive and captured in the ladder, 2 = dead from harvest and reported, and 3 = not observed. $r_t$ is the reporting rate of fishers for the 2-year interval from $t-1$ to $t$.

## Parameterisation by mortality hazard rates

Different cause-specific mortality probabilities ($\Psi$) are not independent of one another; if a certain cause of mortality becomes more prevalent (*e.g.* due to some event or change in the environment), not only will the probability of dying from that cause increase, but the probability of dying from any other cause will decrease at the same time. This confounding complicates inference, but Ergon et al. (2018) have recently shown how it can be avoided by parameterising mark-recapture models with mortality hazard rates instead of probabilities. Doing so not only facilitates biological interpretation of model parameters, but also comes with additional advantages such as easy rescaling of covariate effects across different time intervals and straight-forward calculation of temporal correlations among mortality causes (Ergon et al. 2018). Assuming that the intensities of mortality from different causes remain proportional within time intervals, we can re-define the survival- and mortality probabilities in the trout model using harvest ($m^H$) and other-cause (hereafter "background") mortality hazard rates ($m^O$):

$$S_{n,i,t} = e^{-(m^H_{n,i,t} + m^O_{n,i,t})}$$

$$\Psi^H_{n,i,t} = (1 - S_{n,i,t}) \frac{m^H_{n,i,t}}{m^H_{n,i,t} + m^O_{n,i,t}}$$

$$\Psi^O_{n,i,t} = (1 - S_{n,i,t}) \frac{m^O_{n,i,t}}{m^H_{n,i,t} + m^O_{n,i,t}}$$

# MODEL IMPLEMENTATION

## Individual and temporal variation in parameters

Body size and hydrological conditions are often key determinants of vital rate variation in freshwater fish, including our study population (*e.g.* Carlson et al. 2008, Letcher et al. 2015, Haugen et al. 2008). We thus used individual body size at the beginning of the time-interval and average river discharge during the relevant season as covariates in our model. We further accounted for additional among-year variation in several parameters using normally distributed random effects.

Harvest in our study system has been done mostly using fishing rods or gillnets; the former is often positively correlated with body size (Lewin et al. 2006) while the latter has bell-shaped selectivity curves (Hamley 1975). To account for this, we modelled harvesting mortality hazard rate as a quadratic function of size on the log-scale:

$$\log(m_{i,t}^H) = \log(\mu^H) + \beta_2^H * size_{i,t} + \beta_4^H * size_{i,t}^2 + \epsilon_t^H$$

where $\mu^H$ is the median harvest mortality hazard rate, $\beta_2^H$ and $\beta_4^H$ are slope parameters for linear and quadratic size effects respectively, and $\epsilon_t^H$ are normally distributed random effects. $size_{i,t}$ is the individual length at spawning. As harvest in our study system happens predominantly in the lake, we have not included an effect of river discharge on $m_{i,t}^H$. Harvest is also limited during the spawning migration and as the duration of the spawning migration is also short relative to the two-year interval of analysis, we further assumed that harvest mortality is the same for above- and below-dam spawners (thus omitted the index $n$ here).

Background mortality, on the other hand, is expected to depend on both spawn-

ing location and on river discharge, as above- and below-dam spawners encounter different hydrological conditions during/after spawning and only the former need to pass the dam on their downriver migration. Mortality associated with the spawning migration in general, and passing of the dam in particular, may also depend on body size. We thus modelled background mortality hazard rate as:

$$\log(m^O_{n,i,t}) = \log(\mu^O_n) + \beta^O_{1,n} * discF_t + \beta^O_{2,n} * size_{i,t} + \epsilon^O_t$$

Here the index $n$ indicates the alive state (1 or 2), $discF_t$ is the average discharge during the fall when post-spawned trout are expected to migrate downriver (Oct - Nov), $\beta^O_{1,n}$ and $\beta^H_4$ are slope parameters for size- and discharge effects respectively, and $\epsilon^O_t$ are random effect which are independent of state $n$.

In a previous analysis of a subset of our data, Haugen et al. (2008) found that the probability of using the fish ladder and thus spawning above the dam depended on a complex interplay of individual body size and river discharge. We adopted their basic model structure and extended it by allowing for random among-year variation such that

$$\text{logit}(p_{i,t}) = \text{logit}(\mu^p) + \beta^p_1 * discS_t + \beta^p_2 * size_{i,t} + \beta^p_3 * discS_t * size_{i,t} + \beta^p_4 * size^2_{i,t} + \epsilon^p_t$$

The discharge covariate used here, $discS_t$, represents the average discharge over the summer season when trout undertake their upriver spawning migration (Jul-Oct), while $size_{i,t}$ is the individual length during the upriver spawning migration.

The last main parameter in the model is reporting rate $r$ and this can be expected to vary considerably over a time period of 50 years. To accommodate

this large expected variation, we estimated 5 average reporting rates $\mu^r$, each of which corresponded to a period of 10 years, and further allowed for the same level of random time-variation within each period.

### Extrapolation of individual body size

Body size is a continuous individual trait that changes over time due to growth. Using such a trait as a covariate in a mark-recapture model comes with a missing data problem related to imperfect detection, as body size can only be measured when an individual is actually captured (Pollock 2002). There are several ways to deal with this problem including integrated growth models (Bonner and Schwarz 2006, Letcher et al. 2015) and inter-/extrapolation using other available data or separate models. Here, we adopted the latter approach and used a detailed growth model previously developed for the study population of brown trout (Nater et al. 2018) to impute missing values in the individual size covariate. Specifically, we re-fitted the growth model of Nater et al. (2018) to an extended set of growth data from 5,158 individuals spanning the years 1952 to 2002 and used the resulting parameter estimates to calculate all missing entries in the body size covariate. We chose imputation with an externally run growth model largely due to prohibitive computational demands that would result from analyzing the growth- and mark-recapture data in an integrated framework. The imputation procedure, as well as implementation and results of the growth analysis, are described in more detail in Appendix S5.

## Additional model extensions

In addition to the model structure outlined above, we ran two sets of extended models. First, we accounted for the fact that 3,183 (25%) of the 12,875 individuals in our analysis were reared in a hatchery and stocked into the wild population after smolting. To investigate whether these individuals differed from their wild-born conspecifics, we included an effect of individual origin (stocked vs. wild) on harvest- and background mortality hazard rates ($m^H_{i,t}$ and $m^O_{n,i,t}$), as well as and ladder usage probability ($p_{i,t}$).

Second, we attempted to estimate the temporal correlation between harvest and background mortality hazard rates. To do so, we re-expressed the random effects on the hazard rates such that

$$\begin{aligned} \epsilon^H_t &= \sigma^H_t * \xi^H_t, \qquad & \xi^H_t &\sim \text{Normal}(0,1) \\ \epsilon^O_t &= \xi^O_t + \tau * \xi^H_t, \quad & \xi^O_t &\sim \text{Normal}(0,\sigma^O_t) \end{aligned}$$

where $\sigma^H_t$ and $\sigma^O_t$ are the standard deviations for the random effects on harvest and background mortality hazard rates respectively. The scaling parameter $\tau$ can then be used to calculate the correlation between random effects as $C = \tau/\sqrt{(\sigma^O_t)^2 + \tau^2}$.

## Implementation with Nimble

We implemented the model in a Bayesian framework using the R package `nimble` (de Valpine et al. 2017). To accommodate the 2-year interval of our analysis, we split the data into two sets containing only individuals spawning in even years and in odd years respectively. We then formulated the likelihood for both datasets separately, but analysed them jointly under the assumption that they share the

same intercept-, slope-, and variance parameters.

Markov Chain Monte Carlo (MCMC) sampling of (multistate) mark-recapture models traditionally includes not only the parameters underlying state transition and observation processes but also the latent states of all individuals $i$ at every point in time $t$ (Kéry and Schaub 2011). With extensive datasets (many individuals, long time periods), such hierarchical models can easily end up with a very large number of nodes in the graphical structure, giving rise to prohibitively long MCMC runtimes. This problem is exacerbated by individual covariates, as their inclusion further increases the number of nodes and also makes the use of reduced data representations such as "m-arrays" (*e.g.* Kéry and Schaub 2011) impossible.

To reduce the MCMC runtime for the model presented here, we implemented a custom likelihood function in `nimble` for use in the hierarchical model. Building on the work of Turek et al. (2016), this custom function analytically integrates over the discrete set of latent states to exactly calculate the likelihood of each capture history, conditional on values of the model parameters. Here, with a finite set of latent states, this integration takes the form of a summation over the latent state values. In doing so, we removed a total of 60,641 latent states from the hierarchical model, thus reducing the dimension of the posterior distribution (and equivalently the MCMC sampling problem) by that same number. This also serves to improve the MCMC mixing of the remaining posterior dimensions, as it no longer relies on MCMC integration over the nuisance dimensions. Specifically, for model parameters $\theta$ and capture histories $y = \{y_1, \ldots, y_n\}$, the posterior distribution is updated according to:

$$p(\theta|y) \propto p(\theta) \prod_{i=1}^{n} p(y_i|\theta),$$

where the likelihood $p(y_i|\theta)$ of capture history $y_i$ is calculated using the custom likelihood function, and $p(\theta)$ is the prior specification. Our implementation extends that of Turek et al. (2016) by incorporating individual-specific covariates (in this case, body length) into the likelihood calculation. In addition, to further speed up computation time, our custom implementation strictly uses linear calculations in lieu of the matrix operations used in Turek et al. (2016). This forgoes the need to construct multi-dimensional arrays for storing state transition and observation probabilities, which were found to be prohibitively large. Using this approach to re-define the model resulted in 5.6- and 31.7-fold increases in minimum MCMC efficiency relative to the latent state model run in `nimble` and `JAGS` respectively. Within `nimble`, re-defining the model also allowed 370 times faster model building, twelve times faster compilation, and a 93% reduction in memory usage relative to the latent state model. For more details on the comparison of the custom distribution and standard approaches, see Appendix S2, as well as the supplementary file `nimbleDHMM.R` for code to define the custom likelihood distribution and to specify the complete multistate mark-recapture model.

For running the model on the trout data we used non-informative priors for all parameters, and made use of `nimble`'s default set of samplers. The MCMC algorithm was run for 25,000 iterations, discarding the first 5,000 samples as burn-in. Analyses were run in `R 3.5.0` using version `0.6-13` of the `nimble` package (NIMBLE Development Team 2018).

# MODEL IDENTIFIABILITY & VALIDATION

With increasing model complexity, and particularly when unobserved states are included, it is not obvious whether all parameters within a multi-state mark-recapture model can be estimated (Cole 2012). Failure to estimate parameters may be due to intrinsic parameter redundancy or data limitations. Using an extended (hybrid) symbolic method (Cole et al. 2010, Cole 2012) implemented in the computer algebra package Maple, we looked at intrinsic parameter redundancy in the above described model including different covariate- and random effect structures. The analyses of parameter redundancy are described in more detail in Appendix S3 and accompanying Maple code is also provided as supplementary material.

Subsequently, we tested the ability of our models to correctly and accurately estimate parameters given the available data. This we did by running the model on simulated even- and odd-year data sets generated using parameter values similar to those obtained from models run on real data. We explored the overall performance of models with independent and correlated random effects on sets of simulated data with the same number of years and similar number of individuals as present in the real data. Additionally, we looked into the sensitivity of model performance to variation in the true value of a potentially problematic parameter, the median background mortality of the unobservable state (below-dam spawners). The setup and results from model tests with simulated data are described in Appendix S4.

# Results

## MODEL IDENTIFIABILITY AND PERFORMANCE

We found that in the absence of random effects the only model structures that were intrinsically identifiable were those where harvest mortality depended on an individual time-varying covariate (*e.g.* body size) and background mortality was either constant or dependent on an environmental covariate (Table S3.1). However, all models (irrespective of covariate structure) became identifiable when random year effects were included on at least harvest mortality hazard or reporting rates (Table S3.1).

When run on simulated data, the independent random effect model produced posterior estimates closely resembling the true parameter values (Appendix S4.2). While there was considerable uncertainty in estimates of some parameters (*e.g.* certain random effect levels, covariate effects on $m_2^O$), true values were always within the central 97% interval of posterior posterior distributions. This was also the case for models with correlated random effects. However, we found the estimation of the coefficient of the random effect correlation ($C$) to be problematic: models tended to correctly predict the sign of the correlation, but uncertainty was very large and prohibited drawing conclusions regarding the actual strength of the correlation (Appendix S4.4).

Posterior distributions for all parameters (including random effect levels) estimated from the real data and using the independent random effect model are plotted in Figures S1.2 to S1.10.

## SIZE-DEPENDENT FISH LADDER USAGE

The probability of using the fish ladder - and thus spawning above the dam - depended strongly on both individual size and river discharge (Figures 3). Intermediate-sized trout (around 550 mm) were most likely to pass the dam under any conditions. Smaller trout were much more likely to pass the dam when river discharge was high, whereas the probability decreased rapidly with length for larger trout irrespective of hydrological conditions. Ladder usage probability fluctuated strongly over time (Figures 5c) and was predicted to be slightly lower for stocked (0.722) than wild-born (0.739) trout (Figures S1.11).

## CAUSE- AND SIZE-DEPENDENT MORTALITY

Median mortality hazard rates were estimated at 0.889 (harvest), 0.238 (background above-dam), and 0.045 (background below-dam) per two years for average-sized trout (670 mm). The resulting probabilities of dying during a 2-year interval due to harvest ($\Psi_n^H$) and due to other causes ($\Psi_n^O$) were 0.533 and 0.143 for above-dam spawners and 0.578 and 0.029 for below-dam spawners. Harvest mortality hazard rate was predicted to be highest for individuals with a length around 500 mm while background mortality hazard rate was substantial only for small to intermediate sized individuals spawning above the dam (up to ∼700mm, Figure 4a). Background mortality hazard rate of below-dam spawners, on the other hand, was predicted to be very low for all except the very largest individuals. Consequently, survival probability increased with length for all trout, but more so for those spawning above the dam (Figure 4b). River discharge was predicted to increase background mortality of above-dam spawners only, but this effect was weak

compared to the effect of length (Figure S1.2). Residual among-year random variation was substantial in both harvest- and background mortality (Figures S1.2 - S1.6), with hazard rates at the 97.5 percentile being 2.86- and 4.85-fold higher than at the 2.5 percentile respectively. No strong time-trends were evident in either mortality cause (Figures 5a & 5b).

Model results did not support differences in harvest- or background mortality due to trout origin: hazard ratios of stocked and wild trout were 0.999 (95% CI [0.846, 1.151]) and 1.081 (95% CI [0.749, 1.427]) for harvest and background mortality respectively (Figures S1.11).

The temporal correlation between harvest and background mortality hazard rates was estimated with large uncertainty and a negative posterior mean of -0.237 (Figure 6).

### TEMPORAL PATTERNS IN REPORTING RATE

Reporting rates varied considerably over time with averages estimated at 0.791 (1966-1976), 0.544 (1977-1986), 0.366 (1987-1996), 0.118 (1997-2006), and 0.101 (2007-2016, Figure S1.2). Within-period among-year variation was estimated at 0.476 (SD on logit scale) and a clear decrease in reporting rates over the 50-year time-period was evident (Figure 5d).

## Discussion

Within populations of animals, individuals can differ greatly in their vulnerability to various sources of mortality. Such differences can arise when mortality causes are related to individual traits such as body size, or when there is heterogeneity in

exposure to certain mortality causes as a consequence of, for example, reproductive state or movement. Accounting for individual differences in cause-specific mortality rates is particularly important when some causes are directly related to human activities, and in this study we investigated factors determining vulnerability to harvest- and background mortality of large brown trout exposed to fishing as well as a hydroelectric dam on their migration route.

We found harvest and background mortality of trout to strongly depend on individual body size. Harvest mortality was highest for intermediate-sized trout and outweighed background mortality for most of the observed range of body sizes. Background mortality of trout spawning above the dam was high for small individuals but decreased rapidly with increasing body size. Survival of above-dam spawners was positively size-dependent as a consequence, possibly indicating a survival cost of passing the dam for small individuals. Survival also generally increased with size for trout spawning below the dam (up to ∼800 mm), but data limitations made direct comparisons with above-dam spawners difficult.

Size-dependent survival is well documented for salmonid fishes, but the direction and strength of size effects vary widely across populations, years, and life history stages for stream-, lake- and marine habitats (Carlson et al. 2008, Drenner et al. 2012). The positive size-dependence of survival found in this study aligns with previous findings for the study population (Haugen et al. 2008). However, unlike the previous analysis, we were able to separate the underlying size-dependent mortality rates with respect to harvest and other causes. The relationship between harvest mortality and trout length was non-linear with a peak mortality at around 500 mm (Figure 4a). This peak is well below the average length in the spawning population (670 mm), indicating that smaller mature fish are harvested dispro-

portionately more in this population. While the bell-shaped relationship between vulnerability and body size is consistent with selectivity curves for gillnets (Hamley 1975), the lack of positive size-dependence may seem surprising given that 43% of the reported captures were due to angling in our system and that vulnerability to angling is usually higher for larger fish (Lennox et al. 2017). Nonetheless, larger fish may be less vulnerable to angling if they had a lower probability of approaching lures due to lower feeding frequency, use of different foraging habitat, or preferred prey characteristics differing from those of employed lures (Lewin et al. 2006, Wilde et al. 2003, Arlinghaus et al. 2008). Alternatively, individual learning or cohort selection may have resulted in individuals that have survived to large sizes being more cautious towards fishing gear ("timdity syndrome", Lennox et al. 2017). Despite the relatively lower harvest mortality of large individuals, however, the risk of dying due to fishing was higher than the risk of dying due to any other cause for most of the observed size range. This suggests fishing as the main source of adult mortality in this population (see Kleiven et al. 2016, for a similar result on Atlantic cod).

Effects of body size on background mortality were predicted to be markedly different for trout spawning above and below the dam (Figure 4a). Among above-dam spawners, smaller individuals were much more likely to die from causes other than harvest relative to larger individuals. Background mortality of small (but not intermediate to large) trout spawning above the dam was also predicted considerably above the levels of natural mortality typically expected for freshwater fish of that size (Lorenzen 1996), indicating that passing the dam itself may come with a survival cost for small individuals. Several candidate mechanisms, operating during different phases of the spawning migration, could be responsible for

such a cost. During upriver migration through the fish ladder, for instance, all trout were trapped and handled. This may increase stress levels (Sharpe et al. 1998, Mäkinen et al. 2000) and cause injuries or even death (Harnish et al. 2011), and smaller individuals may be more vulnerable to these (Brakensiek and Hankin 2007). However, this is unlikely to be the main cause here, as trout found dead within or in close proximity of the dam were usually larger - not smaller - than the average ascending trout (data not shown). During downriver migration after spawning above the dam, trout have to swim through the floodgates or the turbine shaft as they pass the dam again to reach the lake. On many hydroelectric dams - including the Hunderfossen dam - racks are installed in front of turbine intakes to prevent downriver migrating fish from entering and being exposed to high turbine mortality (*e.g.* Fjeldstad et al. 2018, Haraldstad et al. 2018). The effectiveness of such racks varies across species and sizes, but they appear to work relatively well for adult salmonids (Calles et al. 2012). Combining this with our results of negatively size-dependent mortality of above-dam spawning trout may thus indicate that the racks in front of the Hunderfossen turbine indeed protect larger (but not smaller) fish from entering and perishing in the turbine shaft. Finally, it is possible that some survival costs of passing the dam extend beyond the upriver- and downriver passages. Roscoe et al. (2011) found reduced survival of Sockeye salmon (*Oncorhynchus nerka*) that had traversed a dam relative to those that did not and suggested energetic costs of the dam passage as a possible mechanism for this. Additional energetic costs may also arise if passing the dam results in migration delays (Fjeldstad et al. 2018), and particularly if such delays forced individuals to overwinter in the river instead of the lake as has been observed in our population. Since energy reserves scale positively with body size (Peters and Peters 1986) such

energetic costs may be heavier for smaller individuals, possibly contributing to the negatively size-dependent background mortality predicted by the model.

We found a decrease in background mortality with body size only for above- but not below-dam spawners (Figure 4a). Reliably estimating size-dependence in background mortality of below-dam spawners did in fact prove difficult not only because below-dam spawners were unobservable, but also because almost no small- to intermediate-sized trout were spawning below the dam due to strong size dependence in ladder usage probability (Figure 3). As a consequence of this skew in the size-distribution towards larger individuals, model predictions of below-dam background mortality are not very reliable for smaller trout. Similarly, any comparisons of background mortality and survival of same-size above- vs. below-dam spawners will only be informative for a relatively narrow size range ($\sim$ 700 - 900 mm). Within this range, there is considerable overlap in model predictions for above- and below-dam spawners and more detailed studies - possibly involving multi-annual radio- or satellite telemetry - will be necessary to properly quantify size-dependent survival costs of passing the dam.

Over the 50-year study period, there was substantial temporal variation in cause-specific mortality (Figure 5a & b). Fluctuations in harvest mortality are to be expected over such long time-periods both due to among-year differences in harvest pressure (total number of fishers, amount of time spent fishing, *etc.*) and differences in exposure and vulnerability of the fish (due to direct and indirect effects of environmental conditions , Lennox et al. 2017). While background mortality remained relatively low over time, it did show a marked increase around 1997-2001, which coincides with a documented severe disease outbreak in the study population (*Saprolegnia* spp. fungal infections, possibly in combination with or as

a result of ulcerative dermal necrosis, Johnsen and Ugedal 2001). Notably, harvest mortality was also relatively high during this period (and survival consequently quite reduced, Figure S1.12), highlighting the possibility for disease to not only increase background mortality but also affect vulnerability to fishing.

Despite harvest and background mortality increasing simultaneously during the disease outbreak period, models predicted that the correlation between the two mortality causes was more likely to be negative than positive (Figure 6). A negative correlation coefficient indicates compensatory mortality: increased harvest mortality leads to a reduction in background mortality (possibly due to reduced population density). Evidence for compensatory mortality has been found in other fish populations (Allen et al. 1998, Fernández-Chacón et al. 2017, Johnston et al. 2007), and while we acknowledge that the data used here is neither sufficient nor particularly suitable for more in-depth investigations into potential compensatory mortality and its underlying mechanisms, we consider this a promising venue for future research.

The probability of a trout using the fish ladder to pass and spawn above the Hunderfossen dam varied greatly depending on individual body size and river discharge (Figure 3). Consistent with previous results (Haugen et al. 2008), ladder usage probability was predicted to be highest for intermediate-sized trout, and especially larger trout were unlikely to use the fish ladder. Furthermore, small to intermediate-sized trout had an increased probability of using the fish ladder when water flow was relatively high. Both surprisingly low fish ladder usage by large individuals and variable effects of hydrological conditions have been documented in other salmonid populations (Caudill et al. 2007, Jonsson and Jonsson 2002). However, many characteristics influencing attractiveness and efficiency of fish ladders

are site-specific (Fjeldstad et al. 2018), and more detailed studies are necessary to explain the patterns observed in this particular system. Since using the fish ladder is prerequisite to accessing the spawning habitat above the dam and may thus have considerable impacts on population dynamics, further studies should also aim to identify additional environmental and individual factors (*e.g.* temperature, disease status) responsible for the large among-year variation in ladder usage probability (Figure 5c).

While our model predicted no substantial time trends in either mortality components or ladder usage probability, fisher's reporting rate of harvested trout was predicted to have decreased substantially over the 50-year study period (Figure 5d). Separately estimating (harvest) mortality and reporting rate causes problems when analysing tag-recovery data and usually requires auxiliary data (Pollock et al. 2004); by using data from individuals recaptured both alive and dead and allowing for flexible temporal variation in parameters, we were able to not only estimate the average reporting rates but also uncover this striking decrease of reporting rate over time. This is not an uncommon pattern in fish tagging studies (Piccolo et al. 2012) and may have been caused by waning public interest in the study as fishers often received neither personal nor official feedback following the reporting of tags. Separating time-dependent reporting rate from other model parameters also had important consequences for the interpretation of temporal patterns in general. Previously, Haugen et al. (2008) analysed part of this data with a "traditional" tag return model (Brownie et al. 1985) and found the joint probability of being harvested and reported to decrease over time. They interpreted this pattern under the assumption of constant reporting rate and concluded that harvest mortality had decreased over time and background mortality had increased (as they found

no trend in survival estimates). Here, on the contrary, we were able to show explicitly that reporting rate has decreased over time while there was no clear trend in either of the two sources of mortality. This result has important implications for tag recovery studies in general: assumptions of constant reporting rate have to be assessed carefully when drawing conclusions about mortality patterns over time, particularly when there are no rewards or other incentives for reporting tags.

Adult survival and its determinants are understudied but important components of salmonid life history (Drenner et al. 2012), and here we have shown that individual differences in body size influence survival through effects on both harvest- and background mortality, as well as spawning location. A trout's origin, on the other hand, did not substantially influence its survival or probability to migrate past the dam (Figure S1.11). While adverse consequences of hatchery rearing are widely documented in salmonids (*e.g* Einum and Fleming 2001, Fleming and Petersson 2001), these may be most pronounced during early life (McLean et al. 2003). Given that all marked individuals in our study populations have survived up to at least the first spawning migration, the lack of differences between wild-born and stocked trout is thus not unexpected and aligns with findings from other studies focusing on adult fish (Caudill et al. 2007, Thorstad et al. 2007).

While our analyses did include body size, spawning location, and origin, there are other sources of individual heterogeneity that we did not account for here. These include - but are not limited to - disease state, birth/smolt cohort, and sex. Evidence for potential effects of disease state came from the model predictions themselves in the form of lower survival and ladder usage during the time period of a known disease outbreak. Diseased individuals are likely to have higher mortality and possibly compromised reproductive output (Bakke and Harris 1998), but

investigating the effects of disease on the study trout population would require individual-level data on disease states, which is not available. Cohort effects are considered to originate from differences in environmental conditions during early life (Lindström 1999), and have been shown to have long-term consequences for adult survival in stream-dwelling marble trout (*Salmo marmoratus,* Vincenzi et al. 2016). Cohort effects may be less influential on the studied trout, which leave their riverine birth habitat for the large lake after 2-7 years, but we were not able to investigate this here as birth/smolt cohort was only known for a small subset of the population (22%) that had been aged using scales (Aass et al. 2017). Sex differences in size-dependent fish survival are also not uncommon (*e.g.* Haraldstad et al. 2018, Haugen et al. 2007) and sex effects have also attracted attention in the context of migration past hydroelectric dams (Roscoe et al. 2011, Caudill et al. 2007). Information on sex is available for the majority of the marked Hunder trout, but detailed investigations into sex differences in growth, cause-specific mortalities and ladder usage probabilities were beyond the scope of this article.

Another aspect of the present study that would profit from further investigations is among-year variability in cause-specific mortalities and ladder usage, or - more specifically - the factors responsible for it. The only environmental covariate included in our analyses was river discharge, and all other temporal variation (Figure 5) is of unknown origin. Among extrinsic environmental influences, water temperature has been documented to have substantial effects on various aspects of salmonid demography, including survival (Letcher et al. 2015, Jonsson and Jonsson 2002). Indeed, (Haugen et al. 2008) found indications that water temperature positively affected both survival and ladder usage probability in the studied trout population. In this analysis, we refrained from including river and lake temperature as covari-

ates because the available measurement time series do not cover the earlier years of the study. Nonetheless, future efforts to include temperature into the model presented here (possibly as partially observed, latent variables with auxiliary predictors) will certainly be worthwhile, especially given the strong trend of increasing temperature in lake Mjøsa (Hobæk et al. 2012) and the potentially strong impacts of chronic and acute temperature increases on salmonid populations (Hague et al. 2011). Food availability is another factor deserving consideration in future studies. Korman et al. (2017), for example, found prey biomass to be a key driver of growth and survival in a strongly fluctuating population of rainbow trout *Oncorhynchus mykiss*. Unfortunately, no time-series data exists on the abundance of prey fish species in our system, which made investigations impossible in this study. Lack of suitable abundance data on the studied population similarly precluded investigating potential impacts of intra-specific population density, but density dependence in salmonids often occurs primarily during the juvenile and not adult life stages (Jonsson et al. 1998, Vincenzi et al. 2016).

Finally, while the fact that harvest mortality generally outweighs background mortality indicated that fishing has large impacts on this population, the present analysis of adult survival represents only one part of the life cycle of the Hunder trout. It is therefore not sufficient for making inferences about the drivers of changes in abundance and trait dynamics at the population level. However, combining the present model with estimates for growth, reproduction, and early life history in a size structured population model (*e.g.* an integral projection model, Ellner and Rees 2006), will allow to gain a more thorough understanding of the consequences of size-dependent harvest mortality, background mortality, and ladder usage probability, the impacts of among-year variation in vital rates, and the

contributions of stocked trout to the population.

## Conclusion

Multi-state mark-recapture-recovery models are powerful tools for estimating and understanding survival in animal populations that experience mortality from both natural and anthropogenic causes (Schaub and Pradel 2004). Here, we have not only separated harvest- from background mortality but also accounted for individual differences in vulnerability due to body size and migration-related exposure to a hydroelectric dam. Within this framework, we used a recently developed reparameterisation of mark-recovery models using hazard rates instead of survival or mortality probabilities (Ergon et al. 2018). This allowed to estimate body size- and environmental effects on harvest- and background mortalities without confounding them, and provided an intuitive way to also estimate the correlation between two sources of mortality within the mark-recapture model. While formulation of the resulting models in a Bayesian framework was straightforward, the inclusion of body size as an individual time-varying covariate came with substantial computational costs. These we were able to overcome by capitalizing on the flexibility of the novel MCMC sampling compiler `nimble`, and writing a highly efficient custom distribution that is easily applicable for any type of multistate mark-recapture model. Last, but not least, we have shown that identifiability issues that are common to multiple mortality cause mark-recapture-recovery models (Schaub and Pradel 2004) can be overcome through the inclusion of appropriate time random effects. Such random effects can only be estimated when data are collected over a sufficient number of years, and this highlights the importance of investing in the (contin-

ued) collection of individual-based data over long time periods (Clutton-Brock and Sheldon 2010).

# Acknowledgements

This work was supported by the Research Council of Norway through the project SUSTAIN (244647/E10). We thank all individuals and institutions that have been involved in collecting, maintaining, and organizing the mark-recapture-recovery data for their contribution (details in Moe et al. 2018), as well as the Norwegian Water and Energy directorate (NVE) for providing the river discharge time-series. Model fitting was performed in part on the Abel Cluster (University of Oslo and Norwegian Meta-Centre for High Performance Computing).

# Data accessibility

The complete mark-recapture-recovery data set will be made available on the Dryad Digital Repository (DOI to be added) accompanied by a Data Paper (Moe et al. 2018).

# References

Aas, Ø., A. Klemetsen, S. Einum, and J. Skurdal, 2010. Atlantic salmon ecology. John Wiley & Sons.

Aass, P., P. S. Nielsen, and Å. Brabrand, 1989. Effects of river regulation on the

structure of a fast-growing brown trout (*Salmo trutta L.*) population. *Regulated Rivers: Research & Management* **3**:255–266.

Aass, P., A. Rustadbakken, S. J. Moe, E. Lund, and T. Qvenild, 2017. Life-history data on Hunder brown trout (*Salmo trutta*) from lake Mjøsa, Norway. *Freshwater Metadata Journal* **25**:1–11.

Allen, M., L. Miranda, and R. Brock, 1998. Implications of compensatory and additive mortality to the management of selected sportfish populations. *Lakes & Reservoirs: Research & Management* **3**:67–79.

Arlinghaus, R., T. Klefoth, A. Kobler, and S. J. Cooke, 2008. Size selectivity, injury, handling time, and determinants of initial hooking mortality in recreational angling for northern pike: the influence of type and size of bait. *North American Journal of Fisheries Management* **28**:123–134.

Bakke, T. A. and P. D. Harris, 1998. Diseases and parasites in wild Atlantic salmon (*Salmo salar*) populations. *Canadian Journal of Fisheries and Aquatic Sciences* **55**:247–266.

Bonner, S. and C. Schwarz, 2006. An extension of the Cormack–Jolly–Seber model for continuous covariates with application to *Microtus pennsylvanicus*. *Biometrics* **62**:142–149.

Brakensiek, K. E. and D. G. Hankin, 2007. Estimating overwinter survival of juvenile Coho salmon in a Northern California stream: accounting for effects of passive integrated transponder tagging mortality and size-dependent survival. *Transactions of the American Fisheries Society* **136**:1423–1437.

Brownie, C., D. R. Anderson, K. P. Burnham, and D. S. Robson, 1985. Statistical inference from band recovery data. *US Fish and Wildlife Service Resource Publication* **156**.

Calles, O., S. Karlsson, M. Hebrand, and C. Comoglio, 2012. Evaluating technical improvements for downstream migrating diadromous fish at a hydroelectric plant. *Ecological Engineering* **48**:30–37.

Carlson, S. M., E. M. Olsen, and L. A. Vøllestad, 2008. Seasonal mortality and the effect of body size: a review and an empirical test using individual data on brown trout. *Functional Ecology* **22**:663–673.

Caudill, C. C., W. R. Daigle, M. L. Keefer, C. T. Boggs, M. A. Jepson, B. J. Burke, R. W. Zabel, T. C. Bjornn, and C. A. Peery, 2007. Slow dam passage in adult Columbia River salmonids associated with unsuccessful migration: delayed negative effects of passage obstacles or condition-dependent mortality? *Canadian Journal of Fisheries and Aquatic Sciences* **64**:979–995.

Clutton-Brock, T. and B. C. Sheldon, 2010. Individuals and populations: the role of long-term, individual-based studies of animals in ecology and evolutionary biology. *Trends in Ecology & Evolution* **25**:562–573.

Cole, D. J., 2012. Determining parameter redundancy of multi-state mark–recapture models for sea birds. *Journal of Ornithology* **152**:305–315.

Cole, D. J., B. J. Morgan, and D. Titterington, 2010. Determining the parametric structure of models. *Mathematical Biosciences* **228**:16–30.

De Roos, A. M., L. Persson, and E. McCauley, 2003. The influence of size-dependent life-history traits on the structure and dynamics of populations and communities. *Ecology Letters* **6**:473–487.

de Valpine, P., D. Turek, C. J. Paciorek, C. Anderson-Bergman, D. T. Lang, and R. Bodik, 2017. Programming with models: writing statistical algorithms for general model structures with nimble. *Journal of Computational and Graphical Statistics* **26**:403–413.

Devillard, S. and Y. Bray, 2009. Assessing the effect on survival of natal dispersal using multistate capture–recapture models. *Ecology* **90**:2902–2912.

Drenner, S. M., T. D. Clark, C. K. Whitney, E. G. Martins, S. J. Cooke, and S. G. Hinch, 2012. A synthesis of tagging studies examining the behaviour and survival of anadromous salmonids in marine environments. *PloS One* **7**:e31311.

Einum, S. and I. Fleming, 2001. Implications of stocking: ecological interactions between wild and released salmonids. *Nordic Journal of Freshwater Research* **75**:56–70.

Ellner, S. P. and M. Rees, 2006. Integral projection models for species with complex demography. *The American Naturalist* **167**:410–428.

Ergon, T., Ø. Borgan, C. R. Nater, and Y. Vindenes, 2018. The utility of mortality hazard rates in population analyses. *Methods in Ecology and Evolution* **9**:2046–2056.

Fernández-Chacón, A., E. Moland, S. H. Espeland, A. R. Kleiven, and E. M. Olsen, 2017. Causes of mortality in depleted populations of atlantic cod estimated from

multi-event modelling of mark–recapture and recovery data. *Canadian Journal of Fisheries and Aquatic Sciences* **74**:116–126.

Fernández-Chacón, A., E. Moland, S. H. Espeland, and E. M. Olsen, 2015. Demographic effects of full vs. partial protection from harvesting: inference from an empirical before–after control-impact study on atlantic cod. *Journal of Applied Ecology* **52**:1206–1215.

Fjeldstad, H.-P., U. Pulg, and T. Forseth, 2018. Safe two-way migration for salmonids and eel past hydropower structures in Europe: a review and recommendations for best-practice solutions. *Marine and Freshwater Research* **69**:1834–1847.

Fleming, I. and E. Petersson, 2001. The ability of released, hatchery salmonids to breed and contribute to the natural productivity of wild populations. *Nordic Journal of Freshwater Research* pages 71–98.

Fujiwara, M. and H. Caswell, 2001. Demography of the endangered North Atlantic right whale. *Nature* **414**:537.

Hague, M., M. Ferrari, J. Miller, D. Patterson, G. Russell, A. Farrell, and S. Hinch, 2011. Modelling the future hydroclimatology of the lower Fraser River and its impacts on the spawning migration survival of Sockeye salmon. *Global Change Biology* **17**:87–98.

Hamley, J. M., 1975. Review of gillnet selectivity. *Journal of the Fisheries Board of Canada* **32**:1943–1969.

Haraldstad, T., E. Höglund, F. Kroglund, A. Lamberg, E. M. Olsen, and T. O. Haugen, 2018. Condition-dependent skipped spawning in anadromous brown trout (*Salmo trutta*). *Canadian Journal of Fisheries and Aquatic Sciences* **75**:2313–2319.

Harnish, R. A., A. H. Colotelo, and R. S. Brown, 2011. A review of polymer-based water conditioners for reduction of handling-related injury. *Reviews in Fish Biology and Fisheries* **21**:43–49.

Haugen, T. O., P. Aass, N. C. Stenseth, and L. A. Vøllestad, 2008. Changes in selection and evolutionary responses in migratory brown trout following the construction of a fish ladder. *Evolutionary Applications* **1**:319–335.

Haugen, T. O., I. J. Winfield, L. A. Vøllestad, J. M. Fletcher, J. B. James, and N. C. Stenseth, 2007. Density dependence and density independence in the demography and dispersal of pike over four decades. *Ecological Monographs* **77**:483–502.

Hilborn, R. and C. J. Walters, 2013. Quantitative fisheries stock assessment: choice, dynamics and uncertainty. Springer Science & Business Media.

Hobæk, A., J. E. Løvik, T. Rohrlack, S. J. Moe, M. Grung, H. Bennion, G. Clarke, and G. T. Piliposyan, 2012. Eutrophication, recovery and temperature in lake Mjøsa: detecting trends with monitoring data and sediment records. *Freshwater Biology* **57**:1998–2014.

Johnsen, B. U. and O. Ugedal, 2001. Soppinfeksjoner (*Saprolegnia* spp.) på laksefisk i norge - statusrapport. *NINA Oppdragsmelding* **716**:1–34.

Johnston, F. D., J. R. Post, C. J. Mushens, J. D. Stelfox, A. J. Paul, and B. Lajeunesse, 2007. The demography of recovery of an overexploited bull trout, *Salvelinus confluentus*, population. *Canadian Journal of Fisheries and Aquatic Sciences* **64**:113–126.

Jonsson, N. and B. Jonsson, 2002. Migration of anadromous brown trout *Salmo trutta* in a Norwegian river. *Freshwater Biology* **47**:1391–1401.

Jonsson, N., B. Jonsson, and L. Hansen, 1998. The relative role of density-dependent and density-independent survival in the life cycle of Atlantic salmon *Salmo salar*. *Journal of Animal Ecology* **67**:751–762.

Kéry, M. and M. Schaub, 2011. Bayesian population analysis using WinBUGS: a hierarchical perspective. Academic Press.

Kleiven, A. R., A. Fernandez-Chacon, J.-H. Nordahl, E. Moland, S. H. Espeland, H. Knutsen, and E. M. Olsen, 2016. Harvest pressure on coastal Atlantic cod (*Gadus morhua*) from recreational fishing relative to commercial fishing assessed from tag-recovery data. *PLoS One* **11**:e0149595.

Koons, D. N., R. F. Rockwell, and L. M. Aubry, 2014. Effects of exploitation on an overabundant species: the lesser snow goose predicament. *Journal of Animal Ecology* **83**:365–374.

Korman, J., M. D. Yard, and T. A. Kennedy, 2017. Trends in rainbow trout recruitment, abundance, survival, and growth during a boom-and-bust cycle in a tailwater fishery. *Transactions of the American Fisheries Society* **146**:1043–1057.

Lebreton, J.-D., T. Almeras, and R. Pradel, 1999. Competing events, mixtures of information and multistratum recapture models. *Bird Study* **46**:S39–S46.

Lennox, R. J., J. Alós, R. Arlinghaus, A. Horodysky, T. Klefoth, C. T. Monk, and S. J. Cooke, 2017. What makes fish vulnerable to capture by hooks? a conceptual framework and a review of key determinants. *Fish and Fisheries* **18**:986–1010.

Letcher, B. H., P. Schueller, R. D. Bassar, K. H. Nislow, J. A. Coombs, K. Sakrejda, M. Morrissey, D. B. Sigourney, A. R. Whiteley, M. J. O'donnell, et al., 2015. Robust estimates of environmental effects on population vital rates: an integrated capture–recapture model of seasonal brook trout growth, survival and movement in a stream network. *Journal of Animal Ecology* **84**:337–352.

Lewin, W.-C., R. Arlinghaus, and T. Mehner, 2006. Documented and potential biological impacts of recreational fishing: insights for management and conservation. *Reviews in Fisheries Science* **14**:305–367.

Lindström, J., 1999. Early development and fitness in birds and mammals. *Trends in Ecology & Evolution* **14**:343–348.

Lorenzen, K., 1996. The relationship between body weight and natural mortality in juvenile and adult fish: a comparison of natural ecosystems and aquaculture. *Journal of Fish Biology* **49**:627–642.

Mäkinen, T. S., E. Niemelä, K. Moen, and R. Lindström, 2000. Behaviour of gill-net and rod-captured Atlantic salmon (*Salmo salar L.*) during upstream migration and following radio tagging. *Fisheries Research* **45**:117–127.

McLean, J. E., P. Bentzen, and T. P. Quinn, 2003. Differential reproductive success of sympatric, naturally spawning hatchery and wild steelhead trout (*Oncorhynchus mykiss*) through the adult stage. *Canadian Journal of Fisheries and Aquatic Sciences* **60**:433–440.

Moe, S. J., C. R. Nater, A. Rustadbakken, A. Vøllestad, E. Lund, O. Hegge, T. Qvenild, and P. Aass, 2018. A 50-year series of mark-recapture-recovery data of large-sized brown trout from lake Mjøsa, Norway. *in prep.*

Nater, C. R., A. Rustadbakken, T. Ergon, Ø. Langangen, S. J. Moe, Y. Vindenes, L. A. Vøllestad, and P. Aass, 2018. Individual heterogeneity and early life conditions shape growth in a freshwater top predator. *Ecology* **99**:1011–1017.

NIMBLE Development Team, 2018. NIMBLE: MCMC, particle filtering, and programmable hierarchical modeling. R package version 0.6-13.

Peters, R. H. and R. H. Peters, 1986. The ecological implications of body size, volume 2. Cambridge University Press.

Piccolo, J. J., J. R. Norrgård, L. A. Greenberg, M. Schmitz, and E. Bergman, 2012. Conservation of endemic landlocked salmonids in regulated rivers: a case-study from lake Vänern, Sweden. *Fish and Fisheries* **13**:418–433.

Pollock, K. H., 2002. The use of auxiliary variables in capture-recapture modelling: an overview. *Journal of Applied Statistics* **29**:85–102.

Pollock, K. H., H. Jiang, and J. E. Hightower, 2004. Combining telemetry and fisheries tagging models to estimate fishing and natural mortality rates. *Transactions of the American Fisheries Society* **133**:639–648.

Ronget, V., M. Garratt, J.-F. Lemaître, and J.-M. Gaillard, 2017. The 'Evo-Demo' implications of condition-dependent mortality. *Trends in Ecology & Evolution* **32**:909–921.

Roscoe, D., S. Hinch, S. Cooke, and D. Patterson, 2011. Fishway passage and post-passage mortality of up-river migrating sockeye salmon in the Seton River, British Columbia. *River Research and Applications* **27**:693–705.

Sæther, B.-E. and Ø. Bakke, 2000. Avian life history variation and contribution of demographic traits to the population growth rate. *Ecology* **81**:642–653.

Schaub, M. and R. Pradel, 2004. Assessing the relative importance of different sources of mortality from recoveries of marked animals. *Ecology* **85**:930–938.

Servanty, S., R. Choquet, É. Baubet, S. Brandt, J.-M. Gaillard, M. Schaub, C. Toïgo, J.-D. Lebreton, M. Buoro, and O. Gimenez, 2010. Assessing whether mortality is additive using marked animals: a Bayesian state–space modeling approach. *Ecology* **91**:1916–1923.

Sharpe, C. S., D. A. Thompson, H. Lee Blankenship, and C. B. Schreck, 1998. Effects of routine handling and tagging procedures on physiological stress responses in juvenile Chinook salmon. *The Progressive Fish-Culturist* **60**:81–87.

Thorstad, E. B., F. Økland, B. Finstad, R. Sivertsgård, N. Plantalech, P. A. Bjørn, and R. S. McKinley, 2007. Fjord migration and survival of wild and hatchery-reared Atlantic salmon and wild brown trout post-smolts. In *Developments in Fish Telemetry*, pages 99–107. Springer.

Turek, D., P. de Valpine, and C. J. Paciorek, 2016. Efficient Markov chain Monte

Carlo sampling for hierarchical hidden Markov models. *Environmental and Ecological Statistics* **23**:549–564.

Vincenzi, S., M. Mangel, D. Jesensek, J. C. Garza, and A. J. Crivelli, 2016. Within- and among-population variation in vital rates and population dynamics in a variable environment. *Ecological Applications* **26**:2086–2102.

Vindenes, Y. and Ø. Langangen, 2015. Individual heterogeneity in life histories and eco-evolutionary dynamics. *Ecology Letters* **18**:417–432.

Wilde, G. R., K. L. Pope, and B. W. Durham, 2003. Lure-size restrictions in recreational fisheries. *Fisheries* **28**:18–26.

Williams, B. K., J. D. Nichols, and M. J. Conroy, 2002. Analysis and management of animal populations. Academic Press.

# Supporting information

The following supporting information is available for this publication: Appendices S1 - S5.

# Figures

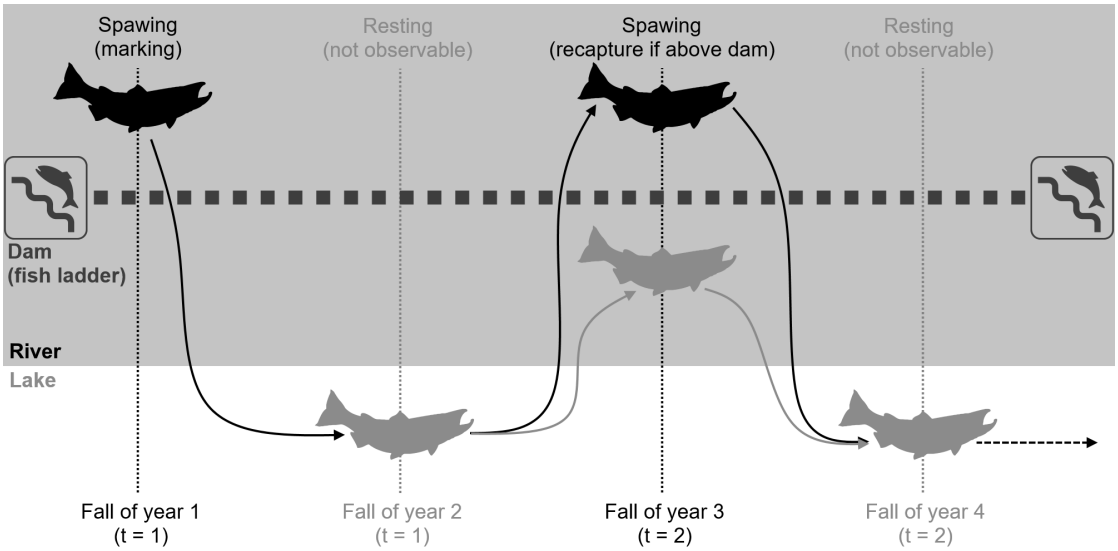


Figure 1: Illustration of the biennial spawning cycle and mark-recapture scheme of the studied trout population. All individuals are marked in the fish ladder while passing the dam on their upriver spawning migration. Two years later they may be recaptured on the next spawning migration, but only if they pass the fish ladder to spawn above the dam. Trout remain in the lake and are unobservable during non-spawning years.

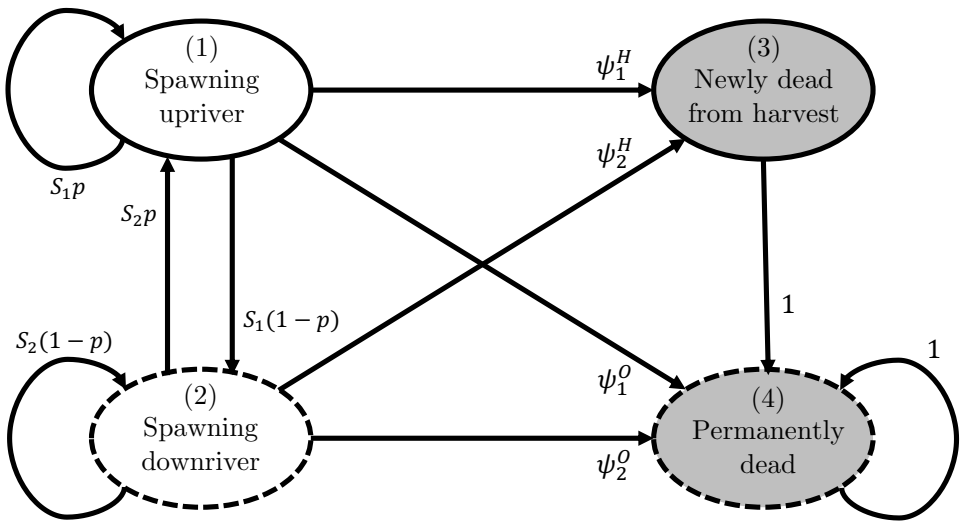


Figure 2: Design of the trout mark-recapture-recovery model (transitions on two-year intervals). White states are alive, grey stages are dead. Solid borders indicate stages that are at least partially observable, whereas dashed borders indicate unobservable stages. $S_n$ = survival probabilities. $\Psi_n^H$ / $\Psi_n^O$ = harvest / background mortality probabilities. $p$ = ladder usage probability. Indices for individual $i$ and time $t$ are omitted here for simplicity.

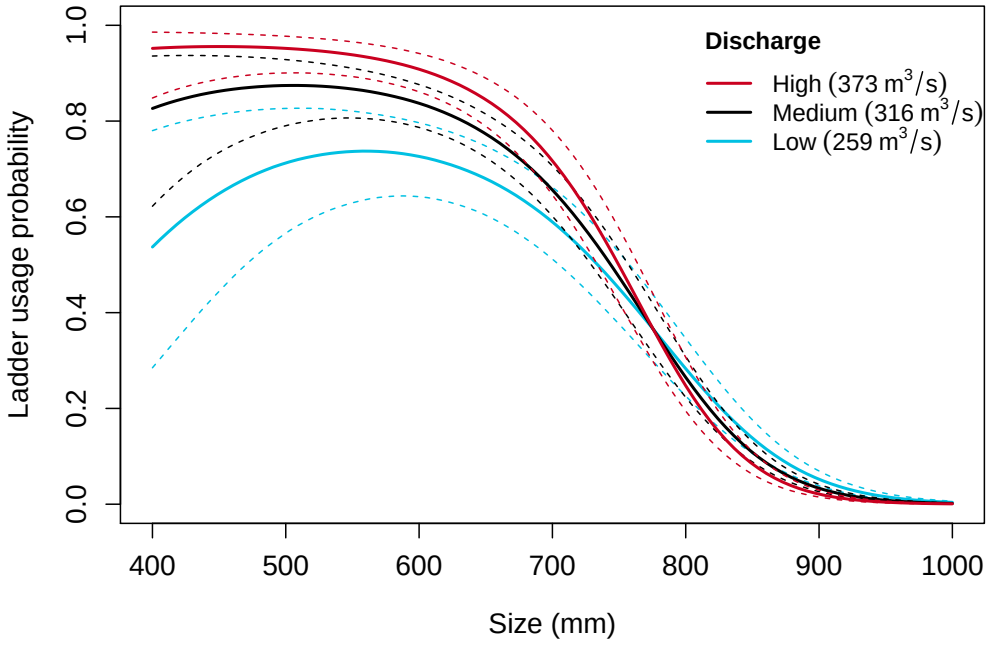


Figure 3: Predictions of the effects of body size on ladder usage probability at different levels of river discharge. Blue = low discharge (mean − SD), black = medium discharge (mean), red = high discharge (mean + SD). Solid lines represent the mean predictions while dashed lines indicate the 95% credibility intervals.

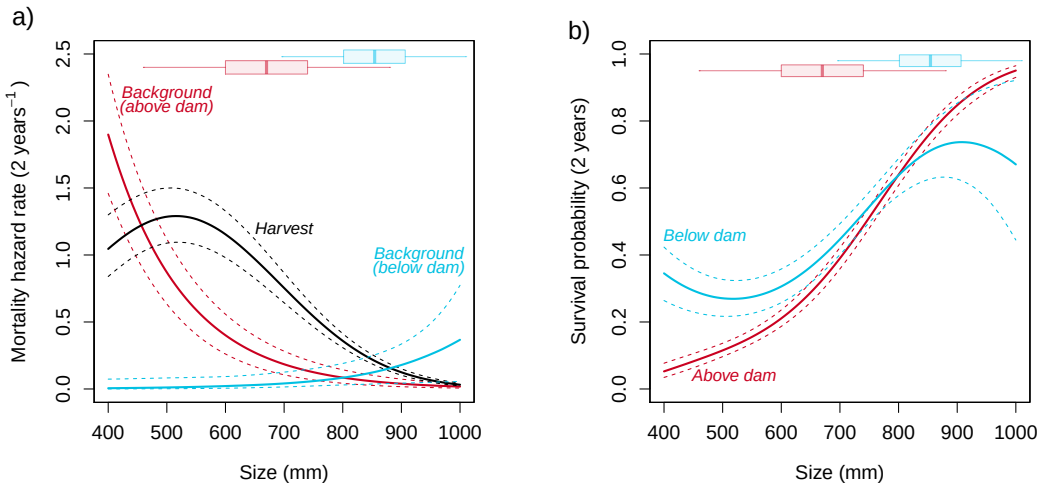


Figure 4: Predictions of the effects of body size on a) harvest and background mortality hazard rates and b) survival probabilities (under consideration of both mortality sources). Red and blue curves apply to individuals that have last spawned above and below the dam respectively. The black curve (harvest) applies to all individuals irrespective of their last spawning location. Solid lines represent the mean predictions while dashed lines indicate the 95% credibility intervals. The boxplot illustrates the informative data range: red = size distribution of individuals captured in the fish ladder (above-dam spawners), blue = simulated size distribution of below-dam spawners after surviving for two years following marking and subsequently not using the fish ladder.

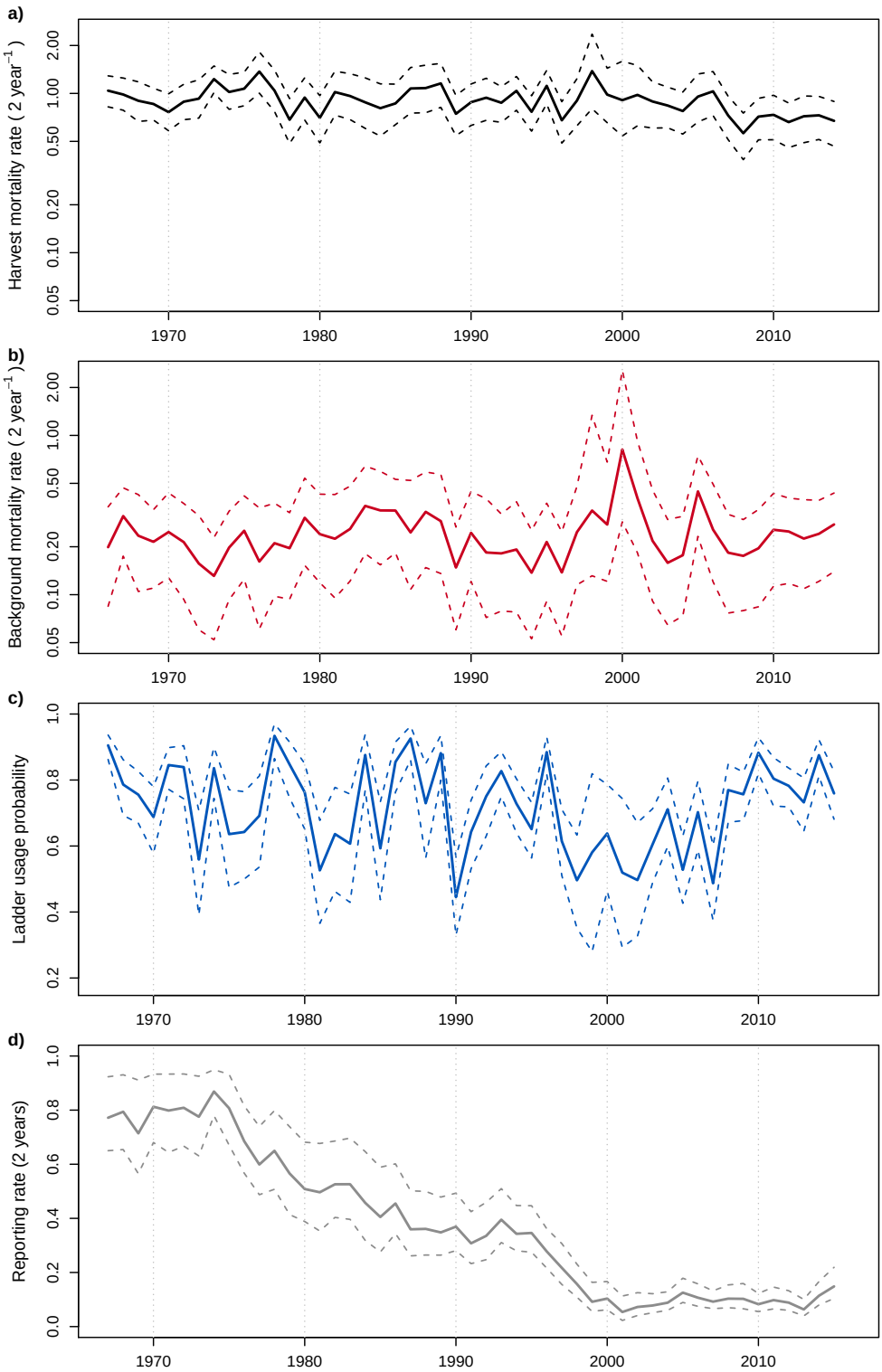


Figure 5: Estimates for time-dependent a) harvest mortality hazard rate, b) background mortality hazard rate (above-dam spawners), c) ladder usage probability, and d) reporting rate (calculated using random variation and discharge effects). Solid lines represent the mean predictions, dashed lines indicate the 95% credibility intervals. y-axes for panels a) and b) are log-scaled.

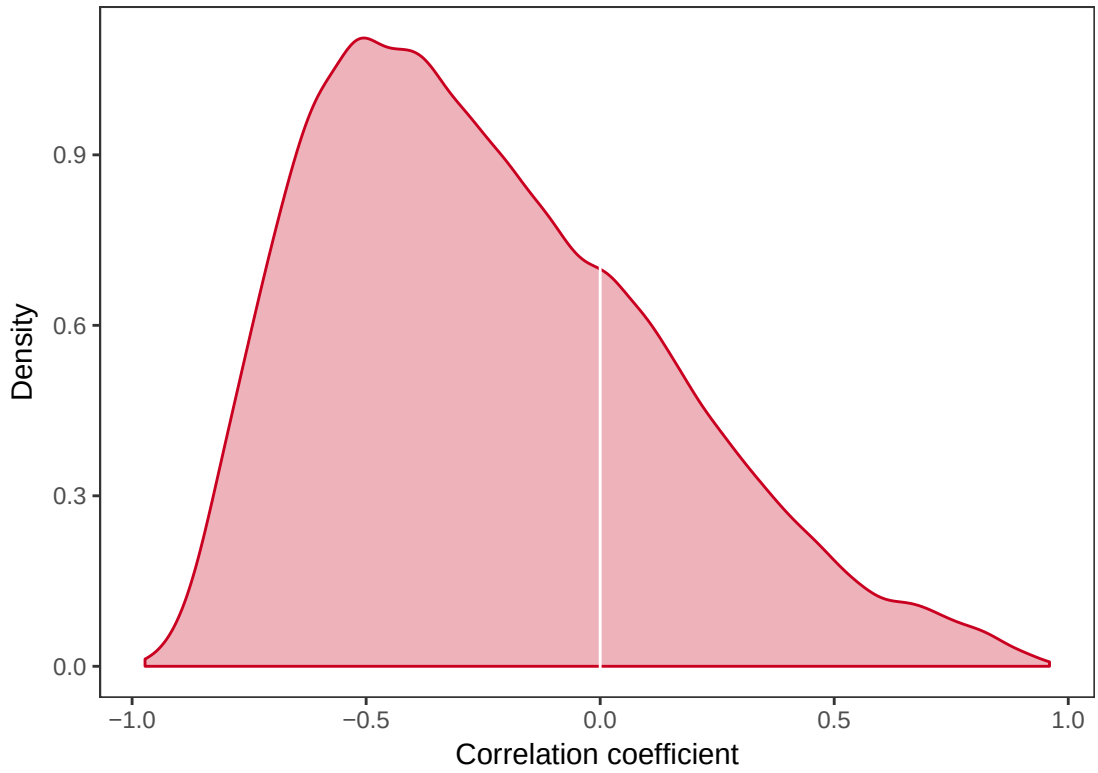


Figure 6: Posterior distributions of coefficient $C$ of the temporal correlation between harvest and background mortality hazard rates estimated by the model.